
The Spike Gating Flow: A Hierarchical Structure Based Spiking Neural Network for Online Gesture Recognition

Zihao Zhao^{1,2}, Yanhong Wang^{1,2}, Qiaosha Zou¹, Tie Xu³, Fangbo Tao³, Jiansong Zhang¹, Xiaoan Wang⁴, C.-J. Richard Shi¹, Junwen Luo^{2,4,*} and Yuan Xie²

¹Fudan University, Shanghai, China

²Alibaba DAMO Academy, Shanghai, China

³Alibaba Group, Hangzhou, China

⁴BrainUp Research Lab, Shanghai, China

Correspondence*:

Junwen Luo

luojunwen@naolubrain.com

ABSTRACT

Action recognition is an exciting research avenue for artificial intelligence since it may be a game changer in the emerging industrial fields such as robotic visions and automobiles. However, current deep learning faces major challenges for such applications because of the huge computational cost and the inefficient learning. Hence, we develop a novel brain-inspired Spiking Neural Network (SNN) based system titled Spiking Gating Flow (SGF) for online action learning. The developed system consists of multiple SGF units which assembled in a hierarchical manner. A single SGF unit involves three layers: a feature extraction layer, an event-driven layer and a histogram-based training layer. To demonstrate the developed system capabilities, we employ a standard Dynamic Vision Sensor (DVS) gesture classification as a benchmark. The results indicate that we can achieve 87.5% accuracy which is comparable with Deep Learning (DL), but at smaller training/inference data number ratio 1.5:1. And only a single training epoch is required during the learning process. Meanwhile, to the best of our knowledge, this is the highest accuracy among the non-backpropagation algorithm based SNNs. At last, we conclude the few-shot learning paradigm of the developed network: 1) a hierarchical structure-based network design involves human prior knowledge; 2) SNNs for content based global dynamic feature detection.

1 INTRODUCTION

Deep Learning (DL) nowadays exerts a substantial impact on a wide range of computer vision tasks such as face recognition (1) and image classifications (2). But it is still facing major challenges when processing information with high dimensional spatiotemporal dynamics such as video action recognition. This is because of: 1) huge computational cost: the deep neural networks have to capture dynamic information across another timing dimensions, which requires significant computational resources for the training stage (3); 2) inefficient learning: events contain significant global dynamic features that are seldomly captured by the DL, but these can be easily recognized by biological systems (4). One promising technology of sparsity (5, 6, 7) can relieve the first issue of the intensive computing to some extent, but the training cost is still

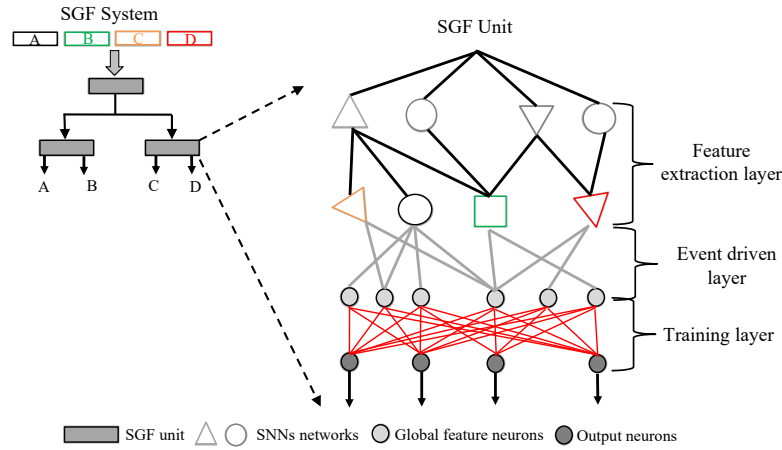


Figure 1. The Spike gating flow system concept. It consists of multiple SGF units. Each SGF unit involves with three layers: 1) a feature extraction layer, 2) an event-driven layer, 3) a training layer. On the top left there is an example of a four-event classification SGF system: A, B, C, D are four event types.

enormous. Recently, Few-Shot Learning (FSL) is proposed to tackle this problem. With prior knowledge, FSL can quickly generalize to new tasks with only a few labeled training samples (8, 9, 10).

Fortunately, Spiking Neural Networks (SNNs) is an alternative candidate to perform spatiotemporal related tasks (11) with few-shot learning capability. By taking the nature characters of computing with time and an event-driven manner, real-world event information will be encoded into spike trains as inputs along with timing frames. With a brain-inspired hierarchical network architecture processing, the output spike patterns are interpreted as inference results via neural decoding methods (e.g. spike timing coding, rank coding, spike count coding). Therefore, this could be an efficient technique for such applications, and another potential path towards the next generation AI (12).

However, employing SNNs for action recognition remains challenging since it lacks an efficient learning algorithm. Recently SNN based learning systems can be classified into three levels: a micro-level, a middle-level and a macro-level system. A micro-level based systems emphasis on utilizing low-level spiking neuron computing characters such as a temporal process and an integration-and-fire manner (13, 14, 15, 16, 17). For instances, (13) proposes an SNN based spatiotemporal Back-Propagation (BP) for a dynamic N-MINST event classifications, the developed algorithm successfully combines spatial and time domain kernels and achieves inference accuracy of 98.78%. Also, (14) illustrates a Convolution Neural Network (CNN) based SNN for gesture classification. By employing an event-driven sensor and a TrueNorth neuromorphic chip, the system shows 178.8mW power consumption and 96.49% accuracy. Meanwhile, A reservoir layer-based SNN utilizes Spike-timing dependent plasticity rule to update weights. Such a novel network can achieve 95% top-3 accuracy on IBM DVS gesture task (14). However, the SNN higher-level computing entities such as attractor dynamics are missed in the system, which results in inefficient learning.

A middle-level system indicates SNNs apply global dynamic behaviors on the learning process (18, 19, 20, 21, 22, 23). A FORCE learning method (23) is able to convert network chaos patterns into a desired one by modifying synaptic weight. Also, a Neural Engine Framework (NEF) develops a method to build dynamic systems based on spiking neurons (19). Such an approach leverages neural non-linearity and weighted synaptic filter as computational resources. Compared to the first type SNNs, a middle-level based SNNs emphasis on global network dynamic rather than individual spiking neurons computing characters.

Therefore, such systems demonstrate much better learning behaviors regarding scalability (20) and model sizes (21) at some particular scenarios.

A macro-level system includes both micro-level and middle-level system's advantages (23, 24). It combines detailed spiking neuron characters and network dynamics together to form a unique learning system. For instance, an olfactory SNN is largely based on the mammalian bulb network architecture, and with a line attractor based neural plasticity rule for online learning odorants (24). The developed system shows great one-shot learning behavior compared to the DL. Meanwhile, (25) proposed a spike-based hybrid plasticity model for solving few-shot learning, continual learning, and fault-tolerance learning problems, it combines both local plasticity and global supervise information for multi-task learning.

In this work we develop a novel macro-level system titled Spike Gating Flow (SGF) for action recognition as shown in Fig. 1. The system consists of multiple SGF units that connect in a hierarchical manner. An SGF unit consists of three layers: 1) a feature extraction layer for global dynamic feature detection; 2) an event-driven layer for generating event global feature vectors; 3) a supervise-based histogram training layer for online learning (redlines in Fig. 1). By employing a Dynamic Vision Sensor (DVS) (26) based gesture dataset (14) as a benchmark, the results demonstrate that the developed SGF has great learning performance: 1) the system can approximately achieve the same level accuracy of 87.5% as the DL but at a training/inference sample ratio 1.5:1 condition. More importantly, only one epoch is required during the training; 2) to our best of knowledge, this is the highest accuracy among the non-BP based SNNs; 3) the system consumes only 9mW and 99KB memory resources on an FPGA board at the inference stage. In summary, the contributions are as follows:

- **Algorithm aspect:** We developed an efficient few-shot learning system for gesture recognition, which behaves like the biological intelligence: few-shot learning, energy efficient and explainable.
- **Application aspect:** the SGF based hardware shows reasonable memory size (99KB) and power consumption (9mW), which is suitable for the edge/end-device scenarios.
- **Learning theory aspect:** We conclude one few-shot learning paradigm: 1) a hierarchical structure-based network design involves with human prior knowledge; 2) SNNs for global dynamic feature detection.

2 THE SPIKE GATING FLOW

The Spike Gating Flow (SGF) is a new learning theory to achieve online few-shot training entities, which is inspired from the Neural Engineering Framework (NEF) (27) and brain assemble theories (28). In brief, the few-shot learning capabilities rely on prior knowledge embedded in the hierarchical architecture and global feature computing. While the online computing benefits from using dynamic spike pattern to encode both data and control flow. Therefore, network different level nodes are served as gates to pass or stop input data information, and spikes are served as gate control signals. We have concluded the key principles of SGF as below:

- **Global feature representations:** Network representations are defined by the combination of different SNNs global movement features rather than pixel local features.
- **Tailor designed hierarchical network structure:** A hierarchical structure-based network for conditional data-path execution. Depending on inputs, SGF unit spike patterns are served as gates command to manipulate data-paths.
- **Histogram based training algorithms:** A global feature-based histogram training adjusts output layer weights based on history information.

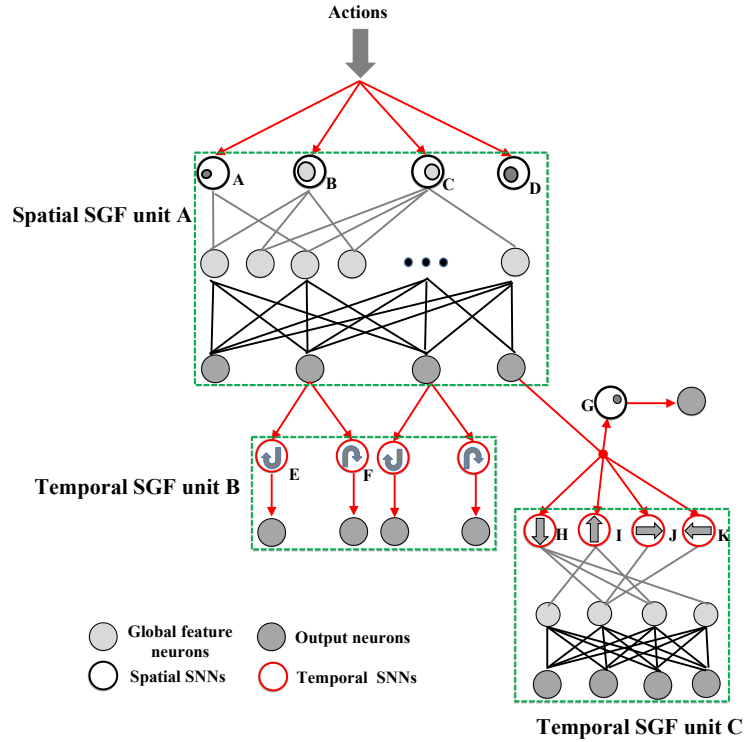


Figure 2. The SGF network architecture. It mainly consists of three SGF units: a spatial SGF unit A and temporal SGF units B and C. A spatial SGF unit A has four SNNs with feature ID index A-D (A: intensive activities at constrained left areas; B: mild activities at plateau left areas; C: mild activities at plateau right areas; D: intensive activities at constrained right areas). A temporal SGF unit B has two SNNs with feature ID index E-F (E: clockwise movement; F: clockwise counter movement). A temporal unit C has four SNNs with feature ID index H-K (H: top-down; I: bottom-up; J: left-right; K: right-left). Also, the developed network has 10 output neurons corresponding to 10 action types.

Based on such principles, we design three SGF units and carefully connect them into a two-level network, particularly for online gesture recognition. Such an architecture can be considered as a pre-designed learning rule, and each SGF unit is designed based on the cell assemblies theories (29), and responses for a unique content based global dynamic features. This aims that the system can manipulate units into a hierarchical level to maximize learning efficiency. As shown at Fig. 2, the top area of the developed network is a spatial SGF unit A, and the bottom areas are temporal SGF units B and C. Typically, a SGF unit consists of three layers: a feature extraction layer, an event-driven layer and a histogram-based training layer. Also, there can be some structure variations of SGF units. For instance, an SGF unit B has a feature extraction layer only.

For an SGF unit computing process, at first a feature extraction layer is to detect events global dynamic features. Each SGF unit has several corresponding spatial SNNs and temporal SNNs, which targets on detecting different global features (features with index A-I are shown at Fig. 2). An SGF unit A has five spatial SNN networks, which responses for detecting spatial features as below: A) intensive activities at a left constrained area; B) mild activities at a left large area; C) mild activities at a right large area; D) intensive activities at right constrained areas; G) intensive activities at a specific constrained area. And an SGF unit B has two temporal SNN networks: E) clockwise movements and F) clockwise counter movements. Particularly, a human prior knowledge of event sequences is introduced here for designing E and F. An SGF unit C has four temporal SNNs: H) up-down movements; I) bottom-up movements;

J) left-right movements and K) right-left movements. The detailed computing mechanisms of SNNs are described at the Section 3 of SNN design.

Next there is an event-driven layer that connects SNNs outputs to the global feature neurons. This layer responses for generating event feature vectors for the next layer training. Typically, an event class will have several feature vectors types due to the spatiotemporal variations. A feature vector can be defined as a combination of active SNNs' feature index, which are represented by connecting active SNNs to one global neuron. Therefore, for each action type, global feature neuron number is equal to the action type feature vector type number.

At last, an SGF unit has a fully connected histogram-based training layer, in which each output neuron connects to its all global feature neurons. After each training trail, feature vector histogram numbers will be updated and converted into corresponding weights. And the conversion is a normalization process. This result of the higher histogram number is, the bigger weights are. At an inference stage, a test sample generated feature vector will be sent into all output neurons for calculating final scores, which follows the equation as below:

$$S_m = \sum_j \frac{(T_j^m * V)}{L_v} \times w_m^j \quad (1)$$

Where S_m is a testing sample score at m^{th} output neuron; w_m is the j^{th} feature vector weights of the m^{th} output neuron; T_j^m is the j^{th} feature vector of the m^{th} output neuron; and V is the feature vector of the testing samples. The symbol $*$ is a bit-wise NOR operation, and L_v is the bit length of the feature vector. The key advances of such a learning algorithm are that each data sample only requires one training time and tiny computational resources for updating weights, which enables rapid online learning behaviors.

A detailed example is illustrated at Fig.3. SNNs with feature index A and D are active at the first training trail, which forms a feature vector $[A - D]$. Hence a corresponding global feature neuron is generated that connects to SNNs with feature index A and D (connected with red lines). And a feature vector histogram is also displayed on the Fig. 3(a) left. After that, the feature vector $[A - D]$ histogram values will be converted into event type A output neuron weights. It is clearly seen that the weight is one since there is only one feature vector type (Fig. 3(a)). Meanwhile a knowledge graph of event type A is produced for quantitative analysis feature vector distributions (Fig. 3(a) right). At a 10th training trail, there are three more feature vectors generated $[A - C, A, C]$ (Fig. 3(b) left red lines). This indicates that there are in total four types of feature vector in the event type A . Identically, corresponding feature vectors histogram numbers $[3, 1, 5, 1]$ will be transformed into event A neuron outputs weights via a training layer. The feature vectors distribution is also updated in the knowledge graph: a vector with green lines indicates histogram values are decreased, while a vector with red lines indicates histogram values are raised. At the end of a 100th training trail, there is no new feature vector appeared, which results of the same global feature neuron number as the 10th training trail. The event A output neuron weights are updated based on the current histogram numbers as a final result. Similarly, the other event types B and C follow the same training procedures.

At the inference stage, a test sample is given into the trained network, which will generate a corresponding test feature vector. And it will go through all the output neurons to calculate the final scores. As shown at Fig. 3(d), there is a trained network which contains three output neurons, whose inference classification result is the maximum one among these output neuron scores.

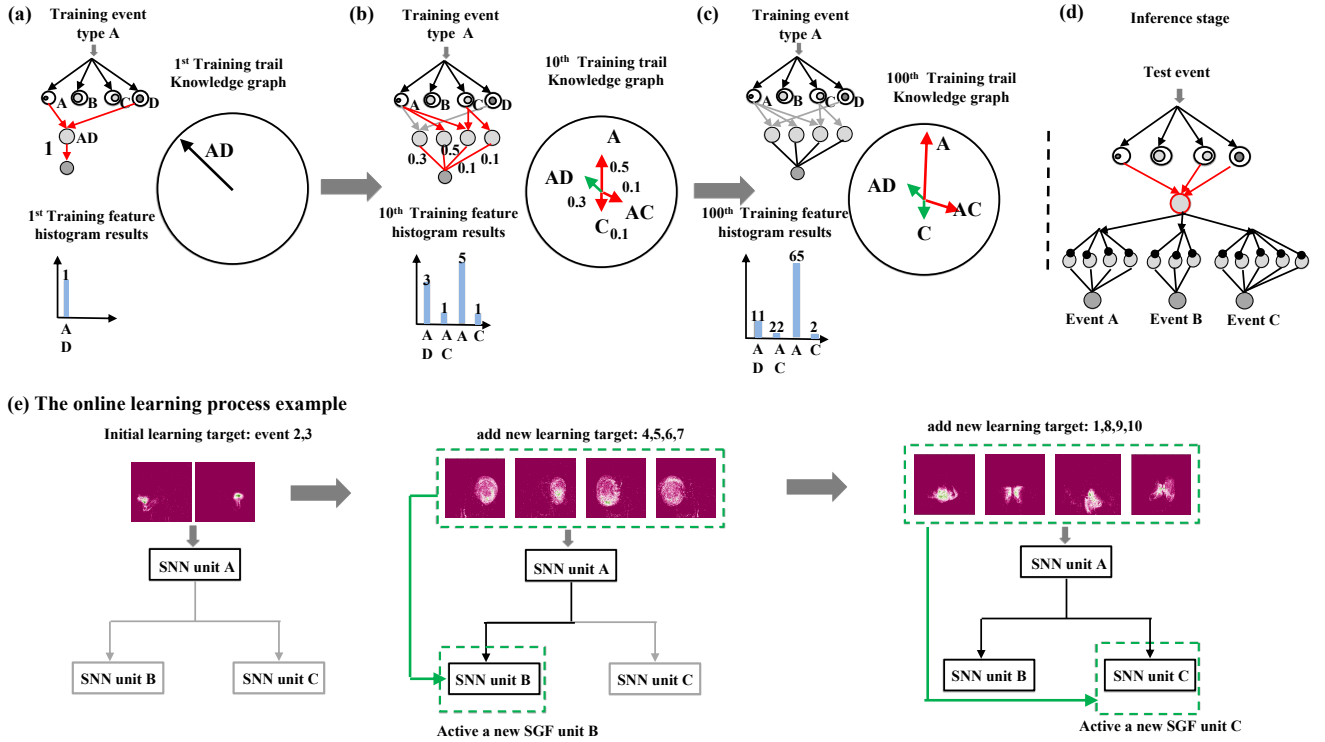


Figure 3. (a)-(d) The histogram-based training example of an event type A; (e) The system online learning process example.

The online learning process example is shown at Fig. 3(e). At an initial stage, event group A [3: right hand wave; 2: left hand wave] is sent into the network for training. Since event group A contains significant spatial features, only a spatial SGF unit A is active and responsible for generating feature vectors. After finishing learning event group A, event group B [4: right arm clockwise, 5: right arm counter clockwise, 6: left arm clockwise, 7: left arm counter clockwise] is sent into the network for sequential online learning. Identically, a temporal SGF unit B is active for recognizing clockwise/counter clockwise movements. At last, event group C [1: hand clap, 2: left hand wave, 8: arm rolls, 9: air drum, 10: air guitar] is sent into network that contains complex combinations of vertical and horizontal movements. The rest of SGF unit C is active for learning such features. As it can be seen, the final network architecture varies depending on the learning targets.

3 SNNS DESIGN

We have developed three SNN types that are SpatioTemporal (ST) cores, spatial SNNs and temporal SNNs. An ST core aims to reduce the DVS camera background noise and enhance key spatiotemporal information. Spatial SNNs response for capturing event's spatial features. And temporal SNNs expert on distinguishing object movement directions. By combining these SNNs, a system can have rich representations of various spatiotemporal features for action classifications.

3.1 Spatiotemporal Core

Since a DVS camera has a unique output format, a spatiotemporal core is designed for DVS output preprocessing: 1) to reduce the DVS output noise; and 2) to enhance the key spatiotemporal information.

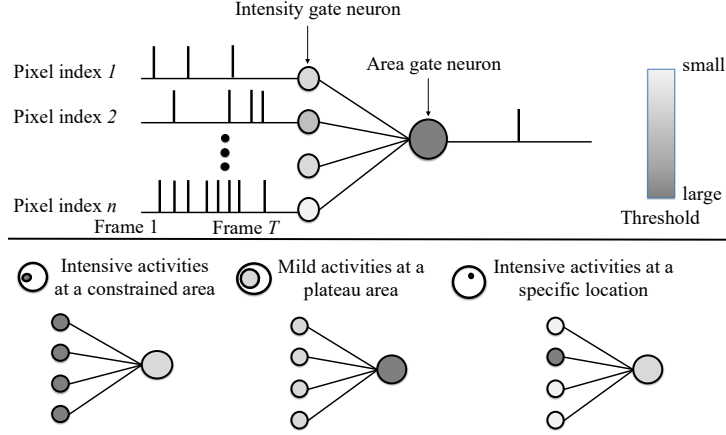


Figure 4. (a) The spatial SNN computing mechanism. The event consists of T frames in total. (b) Examples of three spatial SNNs focus on different global feature detection.

An ST core involves with two-stage computations: a spatial and temporal processing. The mathematical model is as below:

$$ST_m^t = \left[\int_{t-\Delta ST_t}^t \left[\sum_i^{i+\Delta ST_s} d_m^t \right]^{\theta_s} dt \right]^{\theta_t} \quad (2)$$

Where ST_m^t is the outputs of the m^{th} ST core at frame t period; d_m^t is the outputs of the m^{th} DVS sensor pixel at frame t , which equals to -1 or +1; ΔST_s is a ST core spatial detection range. The function $[S]^{\theta_s}$ equals 1 if S over spatial thresholds θ_s . Regarding the temporal computations, ΔST_t is an integration window and θ_t is a temporal threshold. The function $[T]^{\theta_t}$ equals 1 if T is over spatial thresholds θ_t . As a result of this, by adjusting above four parameters $[\Delta ST_s, \theta_s, \Delta ST_t, \theta_t]$, we can configure ST core filtering behaviors properly. In general, each SNN will require a ST core for feature extraction. More details of preprocessing DVS gesture dataset are illustrated in the Results section 4.3.

3.2 Spatial SNNs

A spatial SNN is designed for extracting spatial features based on ST core outputs. The computing mechanism is quite similar with an ST core. However, the major differences rely on 1) the outputs of a spatial SNN are a feature vector; 2) A spatial SNN does not require temporal information, and it accumulates all the frames $[0, T]$ together first and performs spatial computing. The spatial SNN equations are as below:

$$SP_m = \left[\sum_i^{i+\Delta SP_s} \left[\int_{t=0}^{t=T} ST_m^t dST \right]^{\theta_i} \right]^{\theta_a} \quad (3)$$

Where T is the total frame number of an event. ΔSP_s is the detection size and SP_m is the m_{th} spatial SNN outputs. And the outputs can be a single bit or multiple bits. θ_i is an intensity gate neuron threshold, θ_a is an area gate neuron threshold. As Fig. 4(a) depicts, an event consists of T frames is processed by gate neurons first. After that, gate neuron spikes are employed as inputs for area gate neurons.

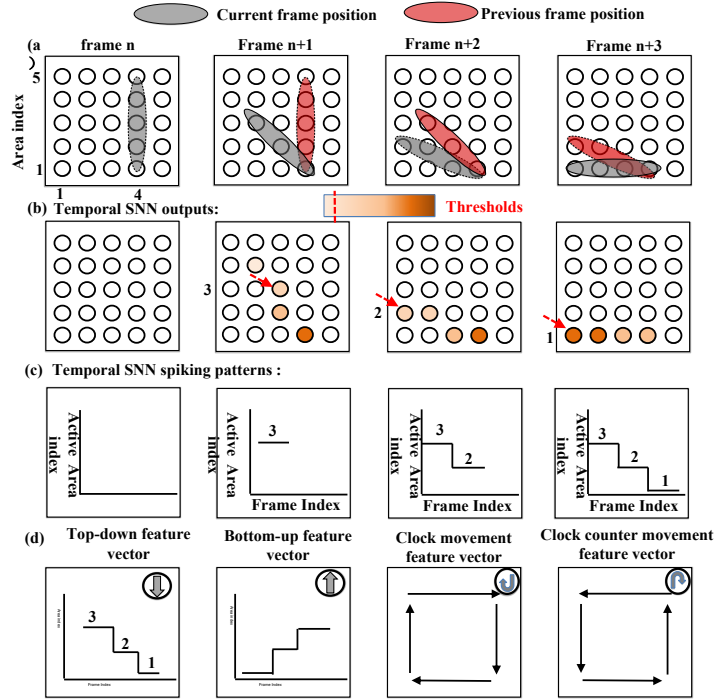


Figure 5. The temporal SNN with feature index H top-down computing mechanism. Also, reference patterns of temporal SNNs with feature index E, F and I are shown at bottom as well.

By adjusting two thresholds' values, three different spatial SNNs can be reconstructed at Fig. 4(b): 1) spatial SNNs with feature index $[A, D]$: intensive activities as a constrained area $[\theta_1 > \theta_2]$; 2) spatial SNNs with feature index $[B, C]$: mild activities at a large area $[\theta_1 < \theta_2]$; and 3) spatial SNNs with feature index $[G]$: intensive activities at a specific location.

3.3 Temporal SNNs

Temporal SNNs are designed for detecting movement directions of an event (e.g., up-down, left-right). The key principle is to encode object's temporal location into temporal neuron spiking patterns. The equation is shown below:

$$TE_m^t = \left[\sum_i^{n^{t-\Delta TE_t}} \left[l_m^t - l_i^{t-\Delta TE_t} \right] \theta_l \right]^{\theta_{te}} \quad (4)$$

Where TE_m^t is the outputs of the m^{th} temporal neuron at frame t ; l_i^t is the location of the i^{th} temporal active neuron at frame t , the location can be either vertical or horizontal information depends on temporal SNN types. ΔTE_t is the comparison frame window; θ_l is the location index threshold, $n^{t-\Delta TE_t}$ is the active neuron number at frame $t - \Delta TE_t$. θ_{te} is the temporal neuron spiking threshold. For each frame, the object location is calculated by selecting the maximum location index of fired neurons. Therefore, objects' temporal movement patterns can be obtained by a combination of generated object locations at each frame, which serve as event temporal feature vectors.

For instance, Fig. 5 shows a temporal SNN with feature index H of detecting top-down movements. At a frame n , an object is vertically located at areas from $[4, 1]$ to $[4, 5]$. Since this is the first frame, a temporal

SNN module index	Spatial SNN			Temporal SNN	
	A/D	B/C	G	E/F	H/I/J/K
Number of OPs	56.0K	63.0K	7.0K	2.1M	27.2K
Model size	304Byte	342Byte	2Byte	240Byte	16Byte
Sub-network number	16	9	2	80	1
Feature vector length	16	18	2	160	2

Table 1. The developed network architecture information.

SNN does not generate activities because there is no comparison reference. At a frame $n + 1$, an object is moving down to a new location as the gray color indicates. Each active neuron (neuron who receives non-zero ST core outputs) will compare its location to all the active neurons at the previous compared frame. If the current neuron location is lower than the previous frame neuron location, the current neuron will receive an input value from the compared neuron. In this top-down case, the location index is defined as the vertical information (Y-axis). The temporal SNN outputs are shown at Fig. 5(b), neurons with dark colors indicate large input values, while neurons with light color indicate limited input values. Neurons then generate a spike when values are above a threshold θ_{te} . After calculating all the frames, the object’s temporal movements are represented by the generated temporal feature vectors. A temporal SNN with feature index H will be active if an object movement temporal feature vector consists with its reference feature vector which is shown at Fig. 5(d) bottom (top-down feature vector). Identically, temporal SNNs with feature index $[I, J, K]$ follow the same computing mechanisms. Corresponding reference feature vectors are also shown at 5(d) bottom. Reference feature vectors which can be pre-defined or learned depends on the task. Particularly, SNNs with feature index $[E, F]$ clockwise and counter clockwise require temporal feature vector timing information that is based on a human prior knowledge. The clockwise counter event temporal pattern sequence is defined as [top-down, left-right, bottom-up, right-left], and the clockwise event temporal pattern sequence is defined as [top-down, right-left, bottom-up, left-right].

4 RESULTS

A DVS gesture dataset (14) (10 different gesture actions) is employed to verify the system performance, since such novel DVS based datasets (30, 31) may exert a significant impact on emerging applications such as automobile and robotics. The training and inference dataset ratio is 1.5:1. The event-driven sensor data preprocessing is followed a standard method (32): an event consists of 50-80 frames, and each frame contains 1000 spikes.

4.1 Network architecture

The detailed network architecture information is shown in Tab. 1. Each SNN type has different sub-network numbers, and each individual shares identical functionalities but with slightly different parameters. SNNs memory sizes and operation numbers are also displayed in the Tab. 1: SNNs with feature index A/D and B/C have the sub-network number 16 and 18, respectively. And the corresponding model sizes are 304 Byte and 342 Byte. Temporal SNNs with feature index E/F have the largest number of OPs: 2.1M. The details of parameter calculation are described at Appendix. A.

4.2 System Accuracy

In Tab. 2, we first compare the developed network with two typical SNN-based gesture recognition networks, a STDP based SNN (33) and a SGD based SNN (34). To the best of our knowledge, our system

Name	Type	Learning method	Learning style	Model information				Training cost		Accuracy
				Size	Diff(\times)	OPs	Diff(\times)	Epoch	T/I ratio	
Reservoir CSNN (33)	SNN	STDP	Offline	3.17MB	88.7 \uparrow	-	-	-	3.8:1	65.0%
Heterogeneity Network (34)	SNN	SGD	Offline	125KB	3.4 \uparrow	-	-	-	3.8:1	82.1%
SCRNN (35)	ANN2SNN	BPTT	Offline	732.34KB	20.0 \uparrow	81.91M	9.9 \uparrow	100	4.1:1	96.59%
SLAYER (36)	ANN2SNN	BP	Offline	1034.8KB	28.3 \uparrow	79.8M	9.6 \uparrow	739	3.8:1	93.64%
Converted SNN (37)	ANN2SNN	BP	Offline	500KB	13.7 \uparrow	651M	78.7 \uparrow	10	3.8:1	96.97%
ConvNet (14)	DNN2SNN	BP	Offline	16.3MB	456 \uparrow	946.82M	114 \uparrow	250	3.8:1	96.5%
PointNet++ (38)	DNN2SNN	BP	Offline	3.50MB	98 \uparrow	440.0M	53.2 \uparrow	250	3.8:1	97.08%
This work	SNN	SGF	Online	36.58KB		8.27M		1	1.5:1	87.5%

"-" indicates the data can not be calculated or not mentioned in the corresponding paper.

Table 2. The comparison between state-of-the-art methods and the proposed SGF network.

indicates the highest accuracy of 87.5% among state-of-the-art non-BP based SNNs. Regarding ANN/DNN converted SNN, the developed network can reach the same level of accuracy as a SLAYER (36), but a slight lower than ConvNet (14) 96.5%, SCRNN (35) 96.59%, Converted SNN (37) 96.97% and PointNet++ (38) 97.08%. However, the network model size can be reduced by 456 times compared to the ConvNet (14), and number of operations can be reduced by 53 times compared to the PointNet++ (38).

Last but not the least, the developed SGF only requires 1 training epoch at a condition of training/inference ratio 1.5:1, which DL networks typical require hundreds training epochs at a condition of 3.8:1. This indicates the system training cost is significantly lower than the DL based networks.

4.3 SNNs Behaviors

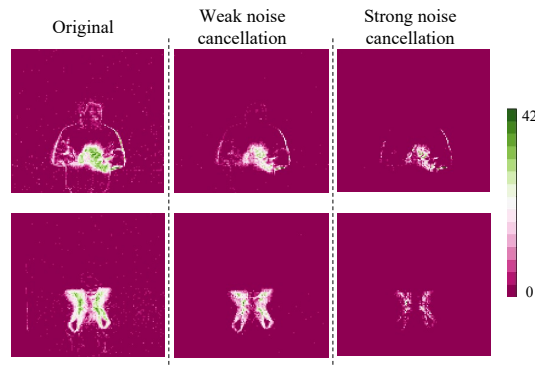


Figure 6. The ST core weak and strong noise cancellation results.

The ST core noise cancellation performance is shown at Fig. 6. At left there are original event pictures of a hand clap and an air drum. Event pictures are obtained via a ST core model process. A color bar on the right displayed spike intensities at each pixel. At middle there are results of an ST core weak noise cancellation (parameters are 1, 1, 2, 2), it is clearly seen that most of sparse noise are disappeared. And at right there are results of an ST core strong noise cancellation (parameters are 1, 1, 6, 5), only most significant features are kept at this case.

Spatial SNNs computing performance is shown at Fig. 7, events of right-hand wave and right hand clock-wise are employed as examples. The results indicate that SNN with feature index A generates a spike for an event of right-hand wave, since it is only sensitive on intensive activities on a constrained area. And

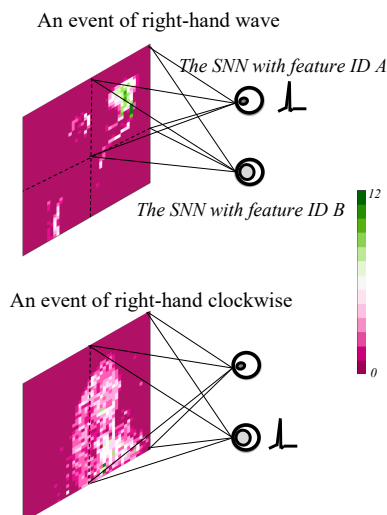


Figure 7. The spatial SNN with feature index A and B results on events of right hand wave and right hand clockwise.

the SNN with feature index B generates a spike for an event of right-hand clockwise, which results from the interests of mild activities on a large area.

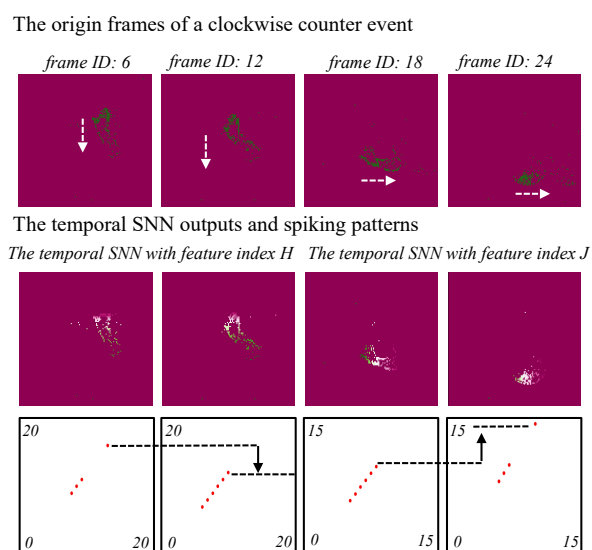


Figure 8. The temporal SNN with feature index E performances.

Temporal SNNs computing performance is shown at Fig. 8. Here we employed an event of clockwise counter as an example. Four original frame information is shown at Fig. 8 top. Corresponding temporal SNNs with feature index H (top-down) and J (left-right) outputs are shown at Fig. 8 middle. It is clearly seen that there is a top-down movement pattern followed by a left-right movement pattern, which are identical to the pattern sequence of clockwise counter event.

4.4 Few-shot learning performance

We also investigate the system's few-shot learning performance. By varying the data ratio between the training and inference stage, results are shown at Fig. 9. Compared to a typical action recognition deep

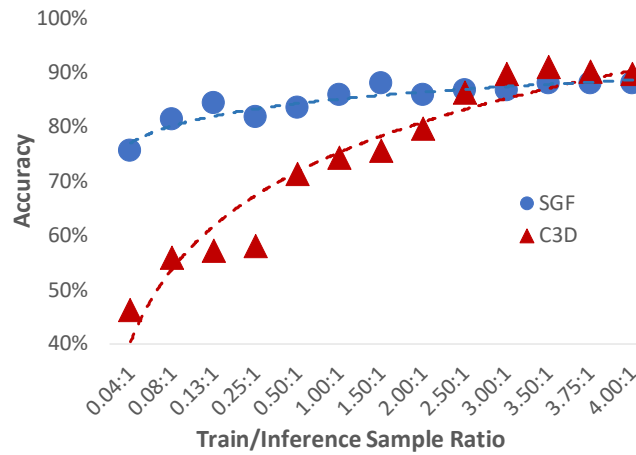


Figure 9. A comparison of the few-shot learning performances on both SGF and C3D networks.

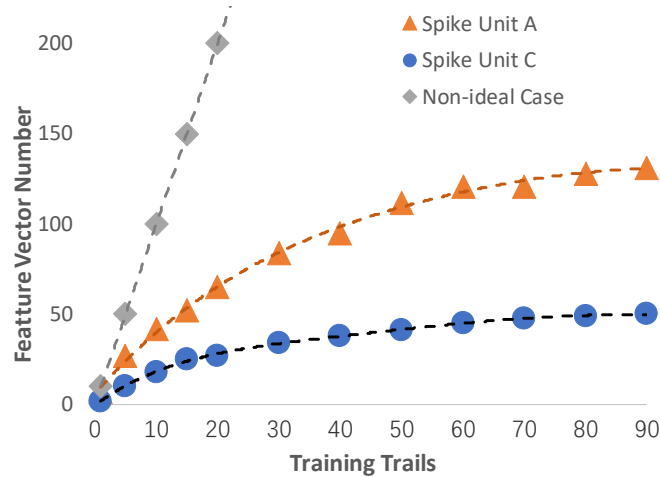


Figure 10. The SNNs design qualities performances. the SGF unit A and C are shown in orange and blue colour, while a non-ideal design case is shown in gray colour.

learning model C3D (39) (red line), the developed SGF illustrates excellent few-shot learning performances. At a training/inference data number ratio 1.5:1 condition, the SGF reached the highest 87.5% accuracy, while the C3D network only has 70% accuracy. However, there is a cross-point at a training/inference data number ratio 3.8:1. The C3D network has reached above 90% accuracy and surpassed the SGF network. In summary, we conclude the key design principles of the developed few-shot learning paradigm: 1) a hierarchical structure-based network design involves with human prior knowledge; 2) SNNs for global dynamic feature detection.

4.5 SNNs design quality

SGF unit design qualities can be evaluated by counting generated feature vector types per training trail. Ideally, the number of feature vector types should be convergent as training trail increases. This indicates that the developed SNNs have strong feature generalization capabilities. As Fig. 10 illustrates, the SGF unit A and C feature vector numbers are convergent gradually as we expected, while a non-ideal design case is also displayed to describe the divergence issues.

4.6 Hardware implementations

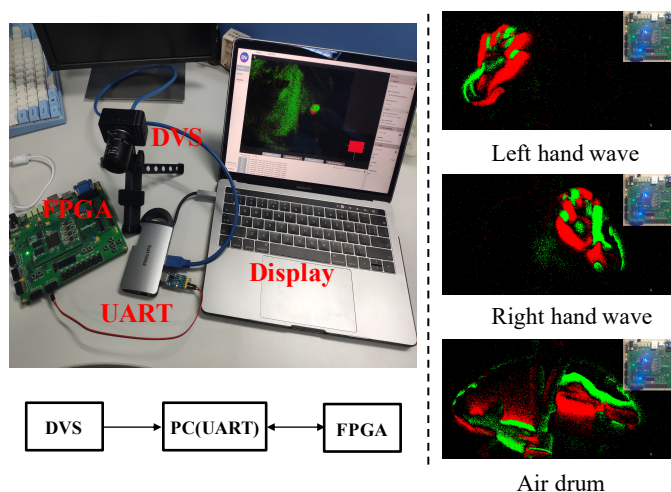


Figure 11. The experimental setup: an SGF inference model is implemented on an FPGA ZedBoard XC7Z020-CLG484-1 for testing system hardware performances.

An SGF inference model is implemented on an FPGA ZedBoard XC7Z020-CLG484-1 for testing system hardware performance. To proof of a concept, the implemented SGF has capabilities of classifying five events. The developed hardware architecture is largely based on (40) with modifications. The system configuration is shown at Fig. 11(a), a DVS camera DAVIS346 (Inivation) is directed connected to a laptop HP Pro Book 430 G6 via a custom designed UART communication protocol. Three event types classification results are shown at Fig. 11 (b): left wave, right wave and air drum. The power consumption is 9mW and memory size is 99KB, which servers as a ideal candidate for edge/end-device applications. The detailed hardware implementations are shown at Appendix B.

5 DISCUSSION

This work presents a novel system titled SGF which has a strong dispersity with the current mainstream deep learning networks. First, we employed a standard DVS gesture classification as a proof of concept. Regarding the training performances, the developed network can achieve the same level of accuracy with the DL under a condition of the training/inference data ratio 1.5:1. More importantly, only one training epoch is required during the learning periods, which significantly reduced the system training cost. Also, in terms of the model complexity, the SGF model size is approximately 379 times smaller than a standard CNN network, and 2.8 times smaller than an SNN. Then we implemented a developed SGF inference model on a tailor designed hardware results of limited power consummations (9mW) and memory resources (99KB). At last we draw conclusions of essential factors achieving few-shot learning paradigms: 1) a hierarchical architecture design encoded with human prior knowledge; 2) SNNs for global feature detections. At last, although the developed system capability has a considerable distance compared to the current DL network, the system shows the essential biological intelligence (e.g. few-shot learning, energy efficient, explainable) at a particular scenario. This may inspire us to design the next generation deep learning algorithms, and also raise a wider discussion among groups of computer hardware architecture, neuroscience and algorithms.

One of the major future work is that the network does not have strong generalization capabilities, which may not be suitable for processing a large-scale dataset (41) (e.g. UCF101). This is due to the network

architecture being tailor designed for the gesture recognition task. Such a design principle of fusing human prior knowledge with SNNs global feature detection introduces a biological intelligence-based system (e.g. few-shot learning, energy efficient and explainable) but with limited flexibility. In the future, we will focus on solving the generalization issue in various technology paths: 1) designing an SNN based Network Architecture Search (NAS) mechanism which similar to the Auto ML (42); 2) introducing a reinforcement learning based agent to generate learning rules that equal to the human prior knowledge (43); 3) utilizing biological brain assembling theories to build a learning logic based architecture (28, 25).

REFERENCES

1. Hu G, Yang Y, Yi D, Kittler J, Christmas WJ, Li SZ, et al. When face recognition meets with deep learning: An evaluation of convolutional neural networks for face recognition. *2015 IEEE International Conference on Computer Vision Workshop, ICCV Workshops 2015, Santiago, Chile, December 7-13, 2015* (IEEE Computer Society) (2015), 384–392. doi:10.1109/ICCVW.2015.58.
2. Krizhevsky A, Sutskever I, Hinton GE. Imagenet classification with deep convolutional neural networks. Bartlett PL, Pereira FCN, Burges CJC, Bottou L, Weinberger KQ, editors, *Advances in Neural Information Processing Systems 25: 26th Annual Conference on Neural Information Processing Systems 2012. Proceedings of a meeting held December 3-6, 2012, Lake Tahoe, Nevada, United States* (2012), 1106–1114.
3. He K, Zhang X, Ren S, Sun J. Deep residual learning for image recognition. *2016 IEEE Conference on Computer Vision and Pattern Recognition, CVPR 2016, Las Vegas, NV, USA, June 27-30, 2016* (IEEE Computer Society) (2016), 770–778. doi:10.1109/CVPR.2016.90.
4. Purves D, Monson BB, Sundararajan J, Wojtach WT. How biological vision succeeds in the physical world. *Proceedings of the National Academy of Sciences* **111** (2014) 4750–4755. doi:10.1073/pnas.1311309111.
5. Liu B, Wang M, Foroosh H, Tappen MF, Pensky M. Sparse convolutional neural networks. *IEEE Conference on Computer Vision and Pattern Recognition, CVPR 2015, Boston, MA, USA, June 7-12, 2015* (IEEE Computer Society) (2015), 806–814. doi:10.1109/CVPR.2015.7298681.
6. Wen W, Wu C, Wang Y, Chen Y, Li H. Learning structured sparsity in deep neural networks. Lee DD, Sugiyama M, von Luxburg U, Guyon I, Garnett R, editors, *Advances in Neural Information Processing Systems 29: Annual Conference on Neural Information Processing Systems 2016, December 5-10, 2016, Barcelona, Spain* (2016), 2074–2082.
7. Liu S, Zhao Z, Wang Y, Zou Q, Zhang Y, Shi CR. Systolic-array deep-learning acceleration exploring pattern-indexed coordinate-assisted sparsity for real-time on-device speech processing. Chen Y, Zhirnov VV, Sasan A, Savidis I, editors, *GLSVLSI '21: Great Lakes Symposium on VLSI 2021, Virtual Event, USA, June 22-25, 2021* (ACM) (2021), 353–358. doi:10.1145/3453688.3461530.
8. Wang Y, Yao Q, Kwok JT, Ni LM. Generalizing from a few examples: A survey on few-shot learning. *ACM Comput. Surv.* **53** (2020). doi:10.1145/3386252.
9. Chen C, Li K, Wei W, Zhou JT, Zeng Z. Hierarchical graph neural networks for few-shot learning. *IEEE Transactions on Circuits and Systems for Video Technology* **32** (2022) 240–252. doi:10.1109/TCSVT.2021.3058098.
10. Sung F, Yang Y, Zhang L, Xiang T, Torr PH, Hospedales TM. Learning to compare: Relation network for few-shot learning. *Proceedings of the IEEE conference on computer vision and pattern recognition* (2018), 1199–1208.
11. Lobo JL, Ser JD, Bifet A, Kasabov NK. Spiking neural networks and online learning: An overview and perspectives. *Neural Networks* **121** (2020) 88–100. doi:10.1016/j.neunet.2019.09.004.

- 12 .Furber SB, Temple S. Neural systems engineering. Fulcher J, Jain LC, editors, *Computational Intelligence: A Compendium* (Springer), *Studies in Computational Intelligence*, vol. 115 (2008), 763–796. doi:10.1007/978-3-540-78293-3_18.
- 13 .Wu Y, Deng L, Li G, Zhu J, Shi L. Spatio-temporal backpropagation for training high-performance spiking neural networks. *Frontiers in Neuroscience* **12** (2018) 331. doi:10.3389/fnins.2018.00331.
- 14 .Amir A, Taba B, Berg DJ, Melano T, McKinstry JL, di Nolfo C, et al. A low power, fully event-based gesture recognition system. *2017 IEEE Conference on Computer Vision and Pattern Recognition, CVPR 2017, Honolulu, HI, USA, July 21-26, 2017* (IEEE Computer Society) (2017), 7388–7397. doi:10.1109/CVPR.2017.781.
- 15 .Lee JH, Delbruck T, Pfeiffer M. Training deep spiking neural networks using backpropagation. *Frontiers in Neuroscience* **10** (2016) 508. doi:10.3389/fnins.2016.00508.
- 16 .Zhang W, Li P. Spike-train level backpropagation for training deep recurrent spiking neural networks. Wallach HM, Larochelle H, Beygelzimer A, d'Alché-Buc F, Fox EB, Garnett R, editors, *Advances in Neural Information Processing Systems 32: Annual Conference on Neural Information Processing Systems 2019, NeurIPS 2019, December 8-14, 2019, Vancouver, BC, Canada* (2019), 7800–7811.
- 17 .Caporale N, Dan Y. Spike timing–dependent plasticity: A hebbian learning rule. *Annual Review of Neuroscience* **31** (2008) 25–46. doi:10.1146/annurev.neuro.31.060407.125639. PMID: 18275283.
- 18 .Eliasmith C. A Unified Approach to Building and Controlling Spiking Attractor Networks. *Neural Computation* **17** (2005) 1276–1314. doi:10.1162/0899766053630332.
- 19 .Bekolay T, Bergstra J, Hunsberger E, DeWolf T, Stewart T, Rasmussen D, et al. Nengo: a python tool for building large-scale functional brain models. *Frontiers in Neuroinformatics* **7** (2014) 48. doi:10.3389/fninf.2013.00048.
- 20 .Voelker A, Kajic I, Eliasmith C. Legendre memory units: Continuous-time representation in recurrent neural networks. Wallach HM, Larochelle H, Beygelzimer A, d'Alché-Buc F, Fox EB, Garnett R, editors, *Advances in Neural Information Processing Systems 32: Annual Conference on Neural Information Processing Systems 2019, NeurIPS 2019, December 8-14, 2019, Vancouver, BC, Canada* (2019), 15544–15553.
- 21 .Chilkuri N, Hunsberger E, Voelker A, Malik G, Eliasmith C. Language modeling using Imus: 10x better data efficiency or improved scaling compared to transformers. *CoRR abs/2110.02402* (2021).
- 22 .Luo J, Chen J. An internal clock based space-time neural network for motion speed recognition. *CoRR abs/2001.10159* (2020).
- 23 .Sussillo D, Abbott L. Generating coherent patterns of activity from chaotic neural networks. *Neuron* **63** (2009) 544–557. doi:https://doi.org/10.1016/j.neuron.2009.07.018.
- 24 .Imam N, Cleland TA. Rapid online learning and robust recall in a neuromorphic olfactory circuit. *CoRR abs/1906.07067* (2019).
- 25 .Wu Y, Zhao R, Zhu J, Chen F, Xu M, Li G, et al. Brain-inspired global-local learning incorporated with neuromorphic computing. *Nature Communications* **13** (2022) 1–14.
- 26 .Posch C, Matolin D, Wohlgenannt R. A QVGA 143 db dynamic range frame-free PWM image sensor with lossless pixel-level video compression and time-domain CDS. *IEEE J. Solid State Circuits* **46** (2011) 259–275. doi:10.1109/JSSC.2010.2085952.
- 27 .Paulin MG. Neural engineering: Computation, representation and dynamics in neurobiological systems: Chris eliasmith, charles anderson; MIT press (december 2003), ISBN: 0262050714. *Neural Networks* **17** (2004) 461–463. doi:10.1016/j.neunet.2004.01.002.

- 28 .Papadimitriou CH, Vempala SS, Mitropolsky D, Collins M, Maass W. Brain computation by assemblies of neurons. *Proceedings of the National Academy of Sciences* **117** (2020) 14464–14472. doi:10.1073/pnas.2001893117.
- 29 .Müller MG, Papadimitriou CH, Maass W, Legenstein R. A model for structured information representation in neural networks of the brain. *eNeuro* **7** (2020). doi:10.1523/ENEURO.0533-19.2020.
- 30 .Gallego G, Delbruck T, Orchard GM, Bartolozzi C, Taba B, Censi A, et al. Event-based vision: A survey. *IEEE Transactions on Pattern Analysis and Machine Intelligence* (2020) 1–1. doi:10.1109/TPAMI.2020.3008413.
- 31 .Hu Y, Liu H, Pfeiffer M, Delbruck T. Dvs benchmark datasets for object tracking, action recognition, and object recognition. *Frontiers in Neuroscience* **10** (2016) 405. doi:10.3389/fnins.2016.00405.
- 32 .Rebecq H, Ranftl R, Koltun V, Scaramuzza D. Events-to-video: Bringing modern computer vision to event cameras. *IEEE Conference on Computer Vision and Pattern Recognition, CVPR 2019, Long Beach, CA, USA, June 16-20, 2019* (Computer Vision Foundation / IEEE) (2019), 3857–3866. doi:10.1109/CVPR.2019.00398.
- 33 .George AM, Banerjee D, Dey S, Mukherjee A, Balamurali P. A reservoir-based convolutional spiking neural network for gesture recognition from DVS input. *2020 International Joint Conference on Neural Networks, IJCNN 2020, Glasgow, United Kingdom, July 19-24, 2020* (IEEE) (2020), 1–9. doi:10.1109/IJCNN48605.2020.9206681.
- 34 .Perez-Nieves N, Leung VCH, Dragotti PL, Goodman DFM. Neural heterogeneity promotes robust learning. *Nature Communications* (2021). doi:10.1038/s41467-021-26022-3.
- 35 .Xing Y, Caterina GD, Soraghan J. A new spiking convolutional recurrent neural network (scrnn) with applications to event-based hand gesture recognition. *Frontiers in Neuroscience* **14** (2020) 590164.
- 36 .Shrestha SB, Orchard G. Slayer: Spike layer error reassignment in time (2018).
- 37 .Kugele A, Pfeil T, Pfeiffer M, Chicca E. Efficient processing of spatio-temporal data streams with spiking neural networks. *Frontiers in Neuroscience* **14** (2020) 439.
- 38 .Qi CR, Su H, Mo K, Guibas LJ. Pointnet: Deep learning on point sets for 3d classification and segmentation. *2017 IEEE Conference on Computer Vision and Pattern Recognition, CVPR 2017, Honolulu, HI, USA, July 21-26, 2017* (IEEE Computer Society) (2017), 77–85. doi:10.1109/CVPR.2017.16.
- 39 .Tran D, Bourdev LD, Fergus R, Torresani L, Paluri M. Learning spatiotemporal features with 3d convolutional networks. *2015 IEEE International Conference on Computer Vision, ICCV 2015, Santiago, Chile, December 7-13, 2015* (IEEE Computer Society) (2015), 4489–4497. doi:10.1109/ICCV.2015.510.
- 40 .Luo J, Coapes G, Mak T, Yamazaki T, Tin C, Degenaar P. Real-time simulation of passage-of-time encoding in cerebellum using a scalable fpga-based system. *IEEE Transactions on Biomedical Circuits and Systems* **10** (2016) 742–753. doi:10.1109/TBCAS.2015.2460232.
- 41 .Soomro K, Zamir AR, Shah M. Ucf101: A dataset of 101 human actions classes from videos in the wild. *ArXiv abs/1212.0402* (2012).
- 42 .He X, Zhao K, Chu X. Automl: A survey of the state-of-the-art. *Knowledge-Based Systems* **212** (2021) 106622. doi:https://doi.org/10.1016/j.knosys.2020.106622.
- 43 .Williams RJ. Simple statistical gradient-following algorithms for connectionist reinforcement learning. *Machine Learning* **8** (1992) 229–256.